

## Important fission product nuclides identification method for simplified burnup chain construction

Go Chiba, Masashi Tsuji, Tadashi Narabayashi, Yasunori Ohoka & Tadashi Ushio

To cite this article: Go Chiba, Masashi Tsuji, Tadashi Narabayashi, Yasunori Ohoka & Tadashi Ushio (2015) Important fission product nuclides identification method for simplified burnup chain construction, Journal of Nuclear Science and Technology, 52:7-8, 953-960, DOI: 10.1080/00223131.2015.1032381

To link to this article: <https://doi.org/10.1080/00223131.2015.1032381>



Published online: 14 Apr 2015.



Submit your article to this journal [↗](#)



Article views: 272



View Crossmark data [↗](#)



Citing articles: 8 View citing articles [↗](#)



## ARTICLE

Physor 2014

### Important fission product nuclides identification method for simplified burnup chain construction

Go Chiba<sup>a\*</sup>, Masashi Tsuji<sup>a</sup>, Tadashi Narabayashi<sup>a</sup>, Yasunori Ohoka<sup>b</sup> and Tadashi Ushio<sup>b</sup>

<sup>a</sup>Division of Energy and Environmental System, Graduate School of Engineering, Hokkaido University, Kita 13 Nishi 8, Kita-ku, Sapporo 060-8628, Japan; <sup>b</sup>Fuel Engineering and Development Department, Nuclear Fuel Industries, Ltd., 950 Asashiro-Nishi 1-chome, Kumatori, Osaka 590-0481, Japan

(Received 19 January 2015; accepted final version for publication 18 March 2015)

A method of identifying important fission product (FP) nuclides which are included in a simplified burnup chain is proposed. This method utilizes adjoint nuclide number densities and contribution functions which quantify the importance of nuclide number densities to the target nuclear characteristics: number densities of specific nuclides after burnup. Numerical tests with light water reactor (LWR) fuel pin-cell problems reveal that this method successfully identifies important FP nuclides included in a simplified burnup chain, with which number densities of target nuclides after burnup are well reproduced. A simplified burnup chain consisting of 138 FP nuclides is constructed using this method, and its good performance for predictions of number densities of target nuclides and reactivity is demonstrated against LWR pin-cell problems and multi-cell problem including gadolinium-bearing fuel rod.

**Keywords:** fission product; burnup chain; adjoint number density; contribution function

#### 1. Introduction

Nuclear fission reactions yield over 1000 fission product (FP) nuclides. Since most of them are neutron-rich isotopes and unstable, they stabilize themselves mainly by  $\beta^-$  decay. Some of them are also converted to different isotopes by neutron–nuclide reactions in an operating nuclear fission reactor. Since these nuclide transmutation processes significantly affect nuclear characteristics of a fission reactor, an accurate numerical simulation of them is required in operation and management of a fission reactor. Since it is unrealistic to explicitly consider all the FPs in an actual core management, a simplified burnup chain consisting of several dozens to about two hundreds important FPs is generally utilized. Usually, identifications of important FPs for a simplified burnup chain have been conducted manually based on experts' knowledge and experiences. As easily expected, such task is quite cumbersome. In the present paper, we propose a new method of identifying important FP nuclides to construct a simplified burnup chain using adjoint nuclide number densities and their associated quantities, contribution functions.

#### 2. Theory

In order to identify important FP nuclides which are required to be considered to accurately calculate specific burnup characteristics of a fission reactor core, we quantify importance of nuclide number density (NND) of FP nuclides during burnup using adjoint NND, which was initially proposed in the framework of the generalized perturbation theory (GPT) for burnup-related nuclear characteristics [1–3]. In the following, we will briefly describe GPT, and then define a quantity which is used to identify important FPs.

Let us consider a nuclear fuel burnup during  $[t_i, t_{i+1}]$ . During this burnup period, neutron flux distribution  $\phi^i$  is assumed to be time-invariant and is calculated by solving the following neutron transport equation:

$$B^i \phi^i = \left( A^i - \frac{1}{k_{\text{eff}}^i} F^i \right) \phi^i = 0, \quad (1)$$

where  $A^i$  and  $F^i$  denote neutron destruction and fission generation operators in  $[t_i, t_{i+1}]$ , respectively, and  $k_{\text{eff}}^i$  is an effective neutron multiplication factor. The neutron

\*Corresponding author. Email: [go\\_chiba@eng.hokudai.ac.jp](mailto:go_chiba@eng.hokudai.ac.jp)

flux  $\phi^i$  is normalized by a reactor power  $P^i$ , which is constant during the burnup period, as

$$\begin{aligned} P^i &= \int_{r \in V_f} \sum_j \kappa_j N_j(t_i) \sum_g \sigma_{f,j,g}^i \phi_g^i(r) dr \\ &= \sum_j \kappa_j N_j(t_i) \langle \sigma_{f,j}^i \phi^i \rangle, \end{aligned} \quad (2)$$

where brackets denote the integration over all the energy groups and whole volume of the system,  $V_f$  is a total volume of a fuel region,  $\mathbf{N}(t_i)$  and  $N_j(t_i)$  denote a NND vector and its  $j$ th entry (NND of nuclide  $j$ ) at  $t = t_i$ , respectively,  $\kappa_j$  and  $\sigma_{f,j,g}^i$  are an emitted energy by one fission reaction and a microscopic fission cross section in energy group  $g$  of nuclide  $j$ , and  $\phi_g(r)$  is a neutron flux of energy group  $g$  at a spatial position  $r$ . For further simplification, Equation (2) is written as

$$P^i = \mathbf{N}(t_i)^T \mathbf{K}(t_i), \quad (3)$$

where the  $j$ th entry of the vector  $\mathbf{K}$  is defined as  $K_j(t_i) = \kappa_j \langle \sigma_{f,j}^i \phi^i \rangle$ . Note that spatial dependences of microscopic cross sections and nuclide number densities in a fuel region are not considered in this study.

Let us consider how to quantify importance of NND of nuclide  $k$  at  $t_i$ ,  $N_k(t_i)$ , to NND of nuclide  $l$  at  $t_{i+1}$ ,  $N_l(t_{i+1})$ . It can be done by observing a change in  $N_l(t_{i+1})$  due to a change in  $N_k(t_i)$  by direct burnup calculations. Whereas importance of NND of every nuclides at  $t_i$  to NND of an arbitrary nuclide at  $t_{i+1}$  can be calculated with this procedure, it requires a huge number of calculation cases. On the other hand, we can calculate the importance of NND effectively by virtue of GPT as follows.

The nuclide burnup equation is written as

$$\frac{\partial \mathbf{N}(t)}{\partial t} = \mathbf{M}^i \mathbf{N}(t), \quad t_i \leq t \leq t_{i+1}, \quad (4)$$

where  $\mathbf{M}^i$  is a burnup matrix at burnup period  $i$  and an initial condition of  $\mathbf{N}(t_i)$  is given. Let us consider that a change  $\Delta \mathbf{N}(t_i)$  is given to the initial condition. In this case, the operator  $B^i$  in Equation (1) changes, so  $\phi^i$  and  $\mathbf{M}^i$  also change. The burnup equation in this perturbed system is written as

$$\frac{\partial \mathbf{N}'(t)}{\partial t} = \mathbf{M}'^i \mathbf{N}'(t), \quad t_i \leq t \leq t_{i+1}, \quad (5)$$

where  $\mathbf{N}'(t) = \mathbf{N}(t) + \Delta \mathbf{N}(t)$  and  $\mathbf{M}'^i = \mathbf{M}^i + \Delta \mathbf{M}^i$ . If we neglect a higher order term, the following equation is derived from Equations (4) and (5):

$$\frac{\partial \Delta \mathbf{N}(t)}{\partial t} = \Delta \mathbf{M}^i \mathbf{N}(t) + \mathbf{M}^i \Delta \mathbf{N}(t). \quad (6)$$

By multiplying a vector  $\mathbf{w}^T(t)$  to both the sides of the above equation and integrating them over  $[t_i, t_{i+1}]$ , we obtain

$$\begin{aligned} \mathbf{w}^T(t_{i+1}) \Delta \mathbf{N}(t_{i+1}) - \mathbf{w}^T(t_i) \Delta \mathbf{N}(t_i) \\ = \int_{t_i}^{t_{i+1}} \Delta \mathbf{N}^T \left( \frac{\partial \mathbf{w}}{\partial t} + \mathbf{M}^i \mathbf{w} \right) dt + \int_{t_i}^{t_{i+1}} \mathbf{w}^T \Delta \mathbf{M}^i \mathbf{N} dt, \end{aligned} \quad (7)$$

where time dependence of  $\Delta \mathbf{N}$ ,  $\mathbf{w}$  and  $\mathbf{N}$  in the integrals are dropped for simplicity. If we define the vector  $\mathbf{w}$  as a solution to the following equation:

$$\frac{\partial \mathbf{w}(t)}{\partial t} = -\mathbf{M}^i \mathbf{w}(t), \quad t_i \leq t \leq t_{i+1}, \quad (8)$$

and the final condition for  $\mathbf{w}(t_{i+1})$  is given as  $\mathbf{w}(t_{i+1}) = \mathbf{e}_l$ , Equation (7) can be written as

$$\Delta N_l(t_{i+1}) = \mathbf{w}^T(t_i) \Delta \mathbf{N}(t_i) + \int_{t_i}^{t_{i+1}} \mathbf{w}^T \Delta \mathbf{M}^i \mathbf{N} dt. \quad (9)$$

Note that  $\mathbf{e}_l$  is the unit vector in which the  $l$ th entry is unity and the others are zero. The above equation suggests that a change in  $N_l(t_{i+1})$  induced by an arbitrary change in  $\mathbf{N}(t_i)$  can be easily calculated if  $\mathbf{w}$  is calculated in advance and the second term of the right-hand side of Equation (9) can be obtained. Since  $\mathbf{M}^{iT}$  is an adjoint to  $\mathbf{M}^i$ , we rewrite  $\mathbf{w}$  as  $\mathbf{N}^i$  and refer to it as an adjoint nuclide number density (ANND) vector. The ANND is defined for a certain quantity which is in interest,  $N_k(t_{i+1})$  in the above case.

Let us consider how  $\Delta \mathbf{M}^i$ , a change in the burnup matrix due to the perturbation in the initial number density vector, can be calculated with the GPT-based procedure. The perturbation in the initial number density vector gives changes in both neutron flux distribution and multi-group microscopic cross sections during burnup. The latter change, however, is considered negligible since the resonance self-shielding effect in conventional thermal neutron reactors is dominantly affected by the neutron fuel-escape cross section, which is dependent on cross sections in non-fuel regions. Thus, the term  $\Delta \mathbf{M}^i$  can be written as

$$\Delta \mathbf{M}^i = \frac{d\mathbf{M}^i}{d\bar{\phi}^i} \frac{\int_{r \in V_f} \Delta \phi^i(r) dr}{V_f}, \quad (10)$$

where  $\bar{\phi}^i$  is an averaged neutron flux in the fuel region. Then, Equation (9) is written as

$$\begin{aligned} \Delta N_l(t_{i+1}) &= \mathbf{N}^{iT}(t_i) \Delta \mathbf{N}(t_i) \\ &+ \left( \int_{t_i}^{t_{i+1}} \mathbf{N}^{iT} \frac{d\mathbf{M}^i}{d\bar{\phi}^i} \mathbf{N} dt \right) \frac{\int_{r \in V_f} \Delta \phi^i(r) dr}{V_f}. \end{aligned} \quad (11)$$

Here we define the following equation:

$$B^{i\dagger} \Gamma^{i\dagger} = S^i, \quad (12)$$

$$S^i = \begin{cases} \frac{\int_{t_i}^{t_{i+1}} \mathbf{N}^{\dagger T} \frac{d\mathbf{M}^i}{d\phi^i} \mathbf{N} dt}{V_f} - \left( \int_{t_i}^{t_{i+1}} \mathbf{N}^{\dagger T} \tilde{\mathbf{M}}^i \mathbf{N} dt \right) \frac{\sum_j \kappa_j N_j(t_i) \sigma_{f,j}^i}{P^i V_f}, & (r \in V_f), \\ 0, & (r \notin V_f), \end{cases} \quad (13)$$

where  $B^{i\dagger}$  is an adjoint operator to  $B^i$ ,  $\Gamma^{i\dagger}$  is a so-called generalized adjoint neutron flux and  $\tilde{\mathbf{M}}^i$  is a component of a burnup matrix  $\mathbf{M}^i$ , in which all the entries are dependent on  $\phi^i$ . Note that the source  $S^i$  is orthogonal to the neutron flux  $\phi^i$ :

$$\langle S^i \phi^i \rangle = 0. \quad (14)$$

By multiplying  $\Delta\phi^i$  to both the sides of Equation (12) and integrating them over all the energy groups and whole volume, we obtain

$$\begin{aligned} & \left( \int_{t_i}^{t_{i+1}} \mathbf{N}^{\dagger T} \frac{d\mathbf{M}^i}{d\phi^i} \mathbf{N} dt \right) \frac{\int_{r \in V_f} \Delta\phi^i(r) dr}{V_f} \\ &= \left\langle \Gamma^{i\dagger} B^i \Delta\phi^i \right\rangle + P^{i\dagger} \frac{\sum_j \kappa_j N_j(t_i) \langle \sigma_{f,j}^i \Delta\phi^i \rangle}{V_f}, \end{aligned} \quad (15)$$

where

$$P^{i\dagger} = \left( \int_{t_i}^{t_{i+1}} \mathbf{N}^{\dagger T} \tilde{\mathbf{M}}^i \mathbf{N} dt \right) \frac{1}{P^i}. \quad (16)$$

The quantity  $P^{i\dagger}$  is referred to as the adjoint power.

The change in the neutron flux  $\Delta\phi^i$  preserves the following equation if we neglect a higher order term:

$$B^i \Delta\phi^i + \Delta B^i \phi^i = 0. \quad (17)$$

Furthermore, since the reactor power is constant during a burnup period, the following relation holds:

$$\begin{aligned} \sum_j \kappa_j N_j(t_i) \langle \sigma_{f,j}^i \Delta\phi^i \rangle &= - \sum_j \kappa_j \Delta N_j(t_i) \langle \sigma_{f,j}^i \phi^i \rangle \\ &= - \Delta \mathbf{N}^T(t_i) \mathbf{K}(t_i). \end{aligned} \quad (18)$$

Using Equations (17) and (18), Equation (15) is rewritten as

$$\begin{aligned} & \left( \int_{t_i}^{t_{i+1}} \mathbf{N}^{\dagger T} \frac{d\mathbf{M}^i}{d\phi^i} \mathbf{N} dt \right) \frac{\int_{r \in V_f} \Delta\phi^i(r) dr}{V_f} \\ &= - \left\langle \Gamma^{i\dagger} \Delta B^i \phi^i \right\rangle - P^{i\dagger} \frac{\Delta \mathbf{N}^T(t_i) \mathbf{K}(t_i)}{V_f}. \end{aligned} \quad (19)$$

Using this equation, Equation (11) is written as

$$\begin{aligned} \Delta N_i(t_{i+1}) &= \left( \mathbf{N}^{\dagger T}(t_i) - \left\langle \Gamma^{i\dagger} \frac{d\mathbf{B}^i}{d\mathbf{N}^T} \phi^i \right\rangle - P^{i\dagger} \frac{\mathbf{K}^T(t_i)}{V_f} \right) \Delta \mathbf{N}(t_i) \\ &= \hat{\mathbf{N}}^{i\dagger T}(t_i) \Delta \mathbf{N}(t_i) = \sum_k \hat{N}_k^i(t_i) \Delta N_k(t_i), \end{aligned} \quad (20)$$

where corrected ANND vector  $\hat{\mathbf{N}}^{i\dagger}$  is defined as

$$\hat{\mathbf{N}}^{i\dagger}(t_i) = \mathbf{N}^{\dagger}(t_i) - \left\langle \Gamma^{i\dagger} \frac{d\mathbf{B}^i}{d\mathbf{N}} \phi^i \right\rangle - P^{i\dagger} \frac{\mathbf{K}(t_i)}{V_f}. \quad (21)$$

If one requires to quantify an effect of a change in NND at the preceding time step  $t_{i-1}$ ,  $\Delta \mathbf{N}(t_{i-1})$ , to NND at  $t_i + 1$ , further calculations should be conducted during the burnup period  $[t_{i-1}, t_i]$  with the final condition of  $\mathbf{N}^{\dagger}(t_i) = \hat{\mathbf{N}}^{i\dagger}(t_i)$ .

In this study, we define a *contribution function* of nuclide  $k$  at  $t = t_i$  to a specific burnup-related nuclear characteristics as  $\text{CF}_k(t_i)$ . If the specific burnup-related quantity is a number density of nuclide  $l$  at  $t = t_l$  (the end of the whole burnup period for example), the contribution function is defined as

$$\text{CF}_k(t_i) = \hat{N}_k^i(t_i) N_k(t_i) / N_l(t_l). \quad (22)$$

The corrected ANND vector is calculated with the corresponding final condition. From the above discussions, we have found that the contribution function can be interpreted as a relative change in  $N_l(t_l)$  when a nuclide  $k$  is ignored at  $t = t_i$  during a burnup calculation. We can quantify the NND importance of all the nuclides during burnup for the NND of the specific nuclide after burnup by this contribution function.

### 3. Procedure of important nuclides identification

As described in the preceding section, the NND importance for specific nuclear characteristics can be quantified by CFs. Thus FP nuclides required to be included in a simplified burnup chain can be identified using CF values. A step-by-step procedure of this identification process is described in the following.

- Step 1: target nuclides, whose NNDs at the specific burnup should be reproduced by a calculation with a simplified burnup chain, are determined.
- Step 2: ANNDs and CFs are calculated for every target nuclides with a reference detailed burnup chain.
- Step 3: a threshold value of CFs,  $\epsilon_{\text{CF}}$ , is determined and nuclides, whose maximum CF values during burnup are larger than this threshold, are identified.
- Step 4: a simplified burnup chain consisting of the identified nuclides is constructed. Fission yields of neglected FP nuclides are added to fission yields

of their daughter nuclides, and paths of radioactive decay are reorganized. If a daughter nuclide B generated by decay or a neutron–nuclide reaction of an identified nuclide A is neglected in the simplified burnup chain and the daughter nuclide B has a decay path to its daughter nuclide C, the nuclide C is treated as a daughter nuclide of the nuclide A, yielded by decay or the neutron–nuclide reaction of the nuclide A.

In order to further reduce the required number of FP nuclides in a simplified burnup chain, we focus on a similarity in ANND between different nuclides. As described above, ANND can be interpreted as an importance of each NDD on a target burnup characteristics. Thus if ANNDs of different nuclides for a specific burnup characteristics are almost the same with each other during whole burnup periods, these two nuclides can be regarded as the same for the target burnup characteristics and we do not have to distinguish these two nuclides. In such a case, we can regard one of these two nuclides as the other (nuclide mixing) and can further reduce the number of required FP nuclides. When such a nuclide pair is detected for one of the target burnup characteristics, the similarity in ANND of these two nuclides is checked for all other target burnup characteristics. If the similarity is not confirmed in different burnup characteristics for which CFs of these two nuclides are larger than the predetermined threshold values, this nuclide mixing is not conducted.

In this nuclide mixing, nuclide with shorter half-life is dropped from the burnup chain and the decay constant of the other nuclide is adjusted as follows. If the radioactive equilibrium can be assumed, the decay constant of the mixed nuclide  $\bar{\lambda}$  can be calculated from decay constants of two nuclides  $\lambda_A$  and  $\lambda_B$  as

$$\bar{\lambda} = \frac{\lambda_A \lambda_B}{\lambda_A + \lambda_B}, \quad (23)$$

since the following equation should be held

$$\lambda_A N_A = \lambda_B N_B = \bar{\lambda} (N_A + N_B). \quad (24)$$

The radioactive equilibrium is assumed, so this treatment is not appropriate for mixing of nuclides with long half-life. In this study, we adopt this procedure if half-lives of two nuclides are less than one day.

Similarity of two ANND is quantified as follows. A burnup-dependent ANND is regarded as a vector. Here let us consider two ANND vectors,  $\mathbf{N}_a^\dagger$  and  $\mathbf{N}_b^\dagger$ . When the following conditions are satisfied, these two vectors are regarded similar to each other:

$$\frac{\mathbf{N}_a^{\dagger T} \mathbf{N}_b^\dagger}{\|\mathbf{N}_a^\dagger\| \|\mathbf{N}_b^\dagger\|} \geq \epsilon_{\text{angle}} \quad (25)$$

and

$$\left| 1 - \frac{\|\mathbf{N}_a^\dagger\|}{\|\mathbf{N}_b^\dagger\|} \right| \leq \epsilon_{\text{length}}, \quad (26)$$

where  $\|\mathbf{N}\|$  denotes the euclidean norm of  $\mathbf{N}$ .

## 4. Numerical result

### 4.1. Verification of the proposed method

The proposed method is tested against burnup characteristics of two light water reactor (LWR) fuel pin-cells. One is a UO<sub>2</sub> fuel cell with 4.1 wt% of U-235 enrichment, and the other is a MOX fuel cell with 10.0 wt% of Pu content. The detailed specification of these fuel cells can be found in reference [4]. First, we calculate reference NNDs of 33 FP nuclides at 45 GWd/t burnup using a detailed burnup chain consisting of over 1000 FP nuclides. The target 33 FP nuclides are chosen from a viewpoint of importance in an actual core management and reactivity prediction. These important 33 FP nuclides are listed as follows: Mo-95, Tc-99, Ru-101, Rh-103, -105, Pd-105, -107, -108, Ag-109, I-135, Xe-131, -135, Cs-133, -134, Pr-141, Nd-143, -145, Pm-147, -148, -148m, -149, Sm-147, -149, -150, -151, -152, Eu-153, -154, -155, Gd-154, -155, -156 and -157.

Fuel depletion calculations of these LWR fuel pin-cells are carried out with a general-purpose deterministic reactor physics calculation code system CBZ being developed at Hokkaido University. Fuel depletion capability of CBZ has been well validated against the post-irradiation examination data [5]. The detailed burnup chain is constructed with the fission yield and decay data given in JENDL FP decay data file 2011 and fission yields data file 2011 [6]. Neutron–nuclide cross sections are taken from JENDL-4.0[7], in which the evaluated data are given to 223 FP nuclides.

Then, we construct a simplified burnup chain which is expected to reproduce the reference NNDs with the proposed method. To do so, we calculate ANNDs and CFs for the NNDs of the above 33 target FP nuclides at 45 GWd/t and identify important FP nuclides using these quantities. The neutron flux and the generalized adjoint neutron flux, which are required to obtain ANNDs and CFs, are calculated with the collision probability method and 107-group cross sections. A burnup chain for heavy nuclides is not simplified.

First let us observe burnup dependent CFs and ANNDs for some nuclear characteristics. **Figures 1** and **2** show CFs of Eu-155, -154, -153, Sm-152 and -151 during burnup to NND of Eu-155 at 45 GWd/t of the UO<sub>2</sub> and MOX cells. Europium-155 is a parent nuclide of Gd-155, which is one of the important nuclides in the burnup credit application to spent nuclear fuel criticality safety management. Contribution of Sm-151 to the Eu-155 NND after burnup is not negligible even though Sm-151 is located far from Eu-155 in a bur-

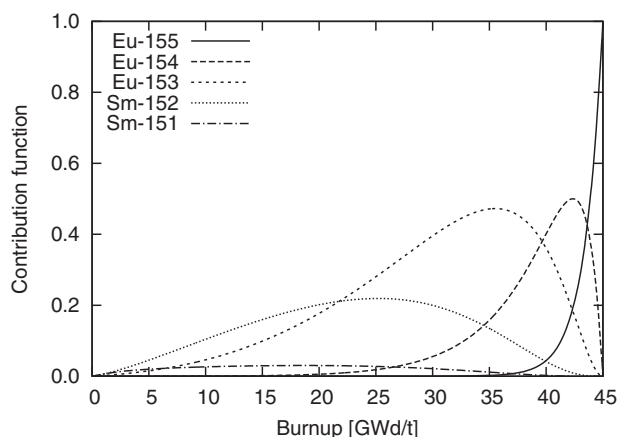


Figure 1. Contribution functions of several FP nuclides to Eu-155 number density after burnup in UO<sub>2</sub> cell.

nup chain. Differences in ANNDs between different fuel cells come from a difference in fission yield values between U-235 and Pu-239 and a difference in neutron flux energy spectrum. As pointed out in reference [8], a neutron flux energy spectrum in a fuel region is much softer and nuclide transmutations by neutron capture reactions are more promoted in the UO<sub>2</sub> cell than in the MOX cell.

Figure 3 shows ANNDs of Eu-153, Sm-153 and Sm-152 during burnup to NND of Eu-154 at 45 GWd/t of the UO<sub>2</sub> cell. Since the burnup-dependent ANNDs of Eu-153 and Sm-153 are quite similar with each other, we can find that these two nuclides, Eu-153 and Sm-153, can be treated as one nuclide to calculate NND of Eu-154 after burnup.

Three simplified burnup chains are constructed by using the proposed important FP identification method with different  $\epsilon_{CF}$  values of  $10^{-3}$ ,  $10^{-4}$  and  $10^{-5}$  and constant values for similarity criteria,  $\epsilon_{angle}$  of 0.95 and  $\epsilon_{length}$  of 0.05. The numbers of FP nuclides included in these constructed burnup chains are 69 in  $\epsilon_{CF} = 10^{-3}$ , 98 in  $\epsilon_{CF} = 10^{-4}$  and 135 in  $\epsilon_{CF} = 10^{-5}$ . The following nu-

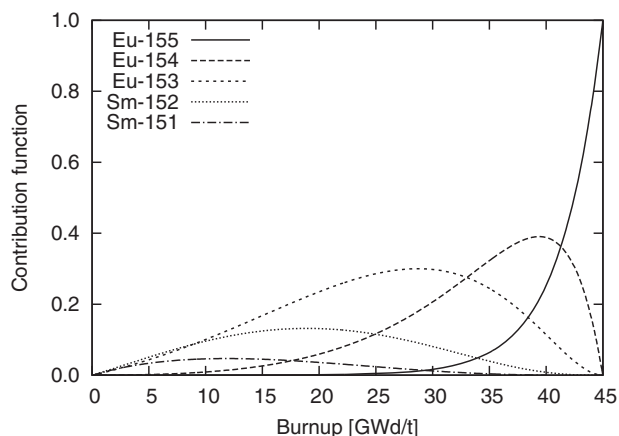


Figure 2. Contribution functions of several FP nuclides to Eu-155 number density after burnup in MOX cell.

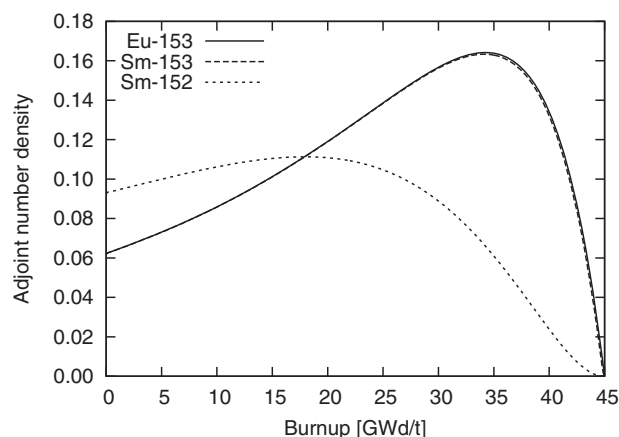


Figure 3. Adjoint number densities of several FP nuclides to Eu-154 number density after burnup.

clide pairs, which can be treated as one mixed nuclide, are detected in the identification process. The first nuclide in each pair is dropped in the present burnup-chain construction:

$$\epsilon_{CF} = 10^{-3}: \text{Tc-105/Ru-105},$$

$$\epsilon_{CF} = 10^{-4}: \text{Mo-105/Tc-105}, \text{Sm-157/Eu-157},$$

$$\epsilon_{CF} = 10^{-5}: \text{Mo-101/Tc-101}, \text{Mo-105/Tc-105}, \text{Sb-131/Te-131}, \text{Ba-141/La-141}.$$

In the simplified burnup chain consisting of 135 FPs, referred to as the 135-chain, Tb-159, Dy-161 and Dy-162 are explicitly treated. Since Tb-159 is generated by neutron capture reactions of gadolinium isotopes, this nuclide and its daughter nuclides are quite important in burnup calculations of gadolinium-bearing fuels. To extend the applicable range of the 135-chain, three isotopes, Tb-160, Dy-160 and Gd-160, are added and a different simplified burnup chain consisting of 138 nuclides is also prepared. The FP nuclides, which are explicitly treated in the 138-chain are listed in Table 1.

Using these four simplified burnup chains, NNDs of 33 target FPs are calculated and compared with the reference values. For a comparison, additional calculations with a burnup chain consisting of 193 FP nuclides implemented in the SRAC code system[9] are also carried out. Maximum values and root-mean-squares (RMS) of reproduction errors of NNDs of the target FP nuclides at 45 GWd/t for the UO<sub>2</sub> and MOX cells are summarized in Table 2. Even with the simplest burnup chain (69-chain), NNDs of most of the target FP nuclides can be reproduced within relative errors of 1%, and the most detailed chain (138-chain) reproduces the target NNDs within 0.03% errors. These results show that the proposed method successfully identifies important FP nuclides to reproduce NNDs of the target nuclides after burnup with simplified burnup chains.

Through observing these numerical results, a natural question might arise; Why are the reproduction errors in the MOX cell smaller than those in the UO<sub>2</sub> cell? There are two possible answers to this question; a difference in fission yield data between U-235 and Pu-239

Table 1. Fission product nuclides explicitly treated in a simplified burnup chain consisting of 138 nuclides.

<i>Se-79</i> , <i>Kr-83</i> , <i>Y-89</i> , <i>-91</i> , <i>-95</i> , <i>Zr-91</i> , <i>-92</i> , <i>-93</i> , <i>-94</i> , <i>-95</i> , <i>-96</i> , <i>Nb-95</i> , <i>-95m</i> , <b>Mo-95</b> , <i>-97</i> , <i>-98</i> , <i>-99</i> , <i>-100</i> , <b>Tc-99</b> , <i>-99m</i> , <i>-101</i> , <i>-105</i> , Ru-100, <b>-101</b> , <i>-102</i> , <i>-103</i> , <i>-104</i> , <i>-105</i> , <i>-106</i> , <b>Rh-103</b> , <i>-103m</i> , <b>-105</b> , <i>-105m</i> , <i>-107</i> , Pd-104, <b>-105</b> , <i>-106</i> , <b>-107</b> , <b>-108</b> , <i>-109</i> , <b>Ag-109</b> , <i>Cd-110</i> , <i>-111</i> , <i>-112</i> , <i>-113</i> , <i>In-115</i> , <i>Sb-121</i> , <i>Te-127m</i> , <i>-129m</i> , <i>-130</i> , <i>-131</i> , <i>-131m</i> , <i>-133m</i> , <i>-135</i> , <i>I-127</i> , <i>-129</i> , <i>-131</i> , <i>-133</i> , <b>-135</b> , <i>Xe-130</i> , <b>-131</b> , <i>-131m</i> , <i>-132</i> , <i>-133</i> , <i>-133m</i> , <i>-134</i> , <b>-135</b> , <i>-135m</i> , <i>-136</i> , <b>Cs-133</b> , <b>-134</b> , <i>-134m</i> , <i>-135</i> , <i>-137</i> , <i>Ba-137</i> , <i>-138</i> , <i>-140</i> , <i>La-139</i> , <i>-141</i> , <i>-143</i> , <i>Ce-140</i> , <i>-141</i> , <i>-142</i> , <i>-143</i> , <i>-144</i> , <i>-149</i> , <b>Pr-141</b> , <i>-143</i> , <i>-145</i> , <i>-147</i> , <i>-149</i> , <i>Nd-142</i> , <b>-143</b> , <i>-144</i> , <b>-145</b> , <i>-146</i> , <i>-147</i> , <i>-148</i> , <i>-149</i> , <i>-150</i> , <i>-151</i> , <i>-152</i> , <b>Pm-147</b> , <b>-148</b> , <b>-148m</b> , <b>-149</b> , <i>-151</i> , <b>Sm-147</b> , <i>-148</i> , <b>-149</b> , <b>-150</b> , <b>-151</b> , <b>-152</b> , <i>-153</i> , <i>-154</i> , <i>-155</i> , <i>-156</i> , <i>-157</i> , <i>Eu-151</i> , <i>-152</i> , <b>-153</b> , <b>-154</b> , <b>-155</b> , <i>-156</i> , <i>-157</i> , <i>Gd-152</i> , <i>-153</i> , <b>-154</b> , <b>-155</b> , <b>-156</b> , <b>-157</b> , <i>-158</i> , <i>-160</i> , <i>Tb-159</i> , <i>-160</i> , <i>Dy-160</i> , <i>-161</i> , <i>-162</i>
--

\*Nuclides shown in bold characters are target ones and those shown in *italic* are not included in the 98-chain.

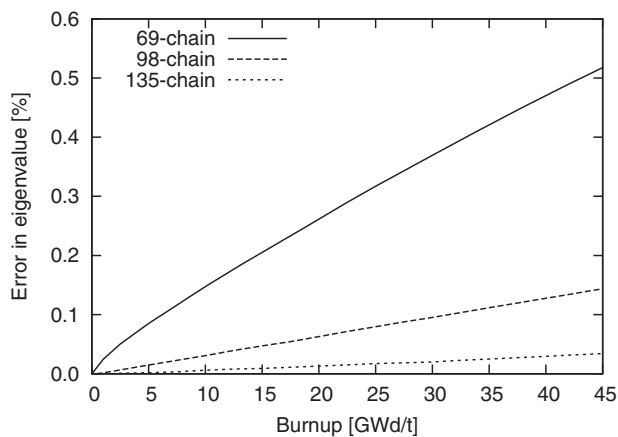
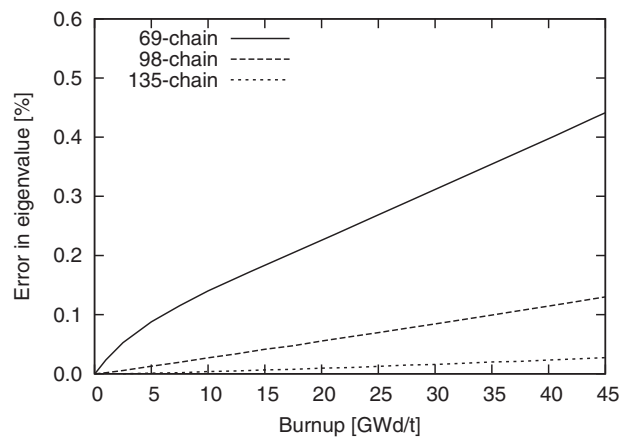
Figure 4. Reproduction errors of eigenvalues during burnup in UO<sub>2</sub> cell.

Figure 5. Reproduction errors of eigenvalues during burnup in MOX cell.

and a difference in neutron flux energy spectra. In order to obtain a clear answer, an additional calculation, in which fission yield data of uranium-235 are replaced by those of plutonium-239, is carried out for the UO<sub>2</sub> cell. Reproduction errors of target NNDs in this case are not significantly different from that in the original UO<sub>2</sub> cell. From these results, we can conclude that the large reproduction errors of the UO<sub>2</sub> cell come from soft neutron flux energy spectrum in comparison with the MOX cell.

Figures 4 and 5 show reproduction errors of eigenvalues (infinite neutron multiplication factor,  $k_{\infty}$ ) during burnup for both the fuel cells. Results obtained with the 138-chain are omitted since those are almost same as ones with the 135-chain. Eigenvalues calculated with the simplified burnup chains are larger than the reference values since neutron capture reactions by some of FP nuclides are neglected in the simplified chains. However, the reproduction errors of eigenvalues

Table 2. Maximum values and root-mean-squares (RMS) of reproduction errors for FP nuclide number densities after burnup.

Burnup chain	UO <sub>2</sub> cell		MOX cell	
	Max. (%)	RMS (%)	Max. (%)	RMS (%)
69-chain	1.019 (Gd-154*)	0.291	0.497 (Gd-154)	0.142
98-chain	0.130 (Gd-157)	0.039	0.042 (Gd-157)	0.011
135-chain	0.025 (Gd-157)	0.007	0.008 (Gd-157)	0.002
138-chain	0.023 (Gd-157)	0.007	0.007 (Gd-157)	0.002
193-chain (SRAC)	0.781 (Gd-154)	0.144	0.331 (Gd-154)	0.070

\*Number densities of these nuclides show maximum reproduction errors.



Table 3. Maximum values and root-mean-squares (RMS) of reproduction errors for FP nuclide number densities after different burnup periods.

Burnup (GWd/t)	UO <sub>2</sub> cell		MOX cell	
	Max. (%)	RMS (%)	Max. (%)	RMS (%)
15	$8.61 \times 10^{-3}$ (Gd-154*)	$2.12 \times 10^{-3}$	$5.54 \times 10^{-3}$ (Gd-154)	$1.66 \times 10^{-3}$
30	$8.43 \times 10^{-3}$ (Gd-157)	$2.54 \times 10^{-3}$	$4.51 \times 10^{-3}$ (Pr-141)	$1.13 \times 10^{-3}$
45	$2.30 \times 10^{-2}$ (Gd-157)	$6.85 \times 10^{-3}$	$6.62 \times 10^{-3}$ (Gd-157)	$1.69 \times 10^{-3}$
60	$4.08 \times 10^{-2}$ (Gd-157)	$1.36 \times 10^{-2}$	$1.52 \times 10^{-2}$ (Gd-157)	$3.42 \times 10^{-3}$

\*Number densities of these nuclides show maximum reproduction errors.

are less than 0.1% when the 135-nuclide burnup chain is used.

#### 4.2. Robustness of simplified burnup chain consisting of 138 fission product nuclides

In the preceding subsection, it has been shown that the 138-chain constructed with the proposed method reproduces quite well NNDs of the target FP nuclides. In the present subsection, robustness of this 138-chain is tested through calculations of the target NNDs at different calculation conditions.

First, reproduction errors of the target NNDs at several burnup periods are quantified. Results are summarized in Table 3. Whereas the 138-chain is constructed to reproduce the target NNDs at 45 GWd/t, those at smaller burnup periods, such as 15 and 30 GWd/t, are also well reproduced by the 138-chain. Reproduction errors of the target NNDs at 60 GWd/t burnup are larger than those at 45 GWd/t, but this is not significant.

Second, reproduction errors of the target NNDs of other UO<sub>2</sub> cells with different U-235 enrichment are quantified. Results are summarized in Table 4. Whereas the 138-chain is constructed to reproduce the target NNDs of the UO<sub>2</sub> cell with 4.1 wt% enrichment, those at other UO<sub>2</sub> cells with different enrichment are also well reproduced by the 138-chain. It is interesting to point out smaller reproduction errors in the UO<sub>2</sub> cell with the 4.7 wt% enrichment than other cases. It can be explained by a difference in neutron flux energy spectrum as already discussed in the preceding section.

Finally, the 138-chain is used in burnup calculation of multi-cell problem including gadolinium-bearing fuel. A 3 × 3 multi-cell system, in which gadolinium-bearing fuel is located at the center position and the others are normal UO<sub>2</sub> fuel with white boundary con-

Table 4. Maximum values and root-mean-squares (RMS) of reproduction errors for FP nuclide number densities after 45 GWd/t burnup in UO<sub>2</sub> cell with different U-235 enrichment.

U-235 enrichment (wt%)	Max. (%)	RMS (%)
3.4	$2.55 \times 10^{-2}$	$8.01 \times 10^{-3}$
4.1	$2.30 \times 10^{-2}$	$6.85 \times 10^{-3}$
4.7	$2.09 \times 10^{-2}$	$6.02 \times 10^{-3}$

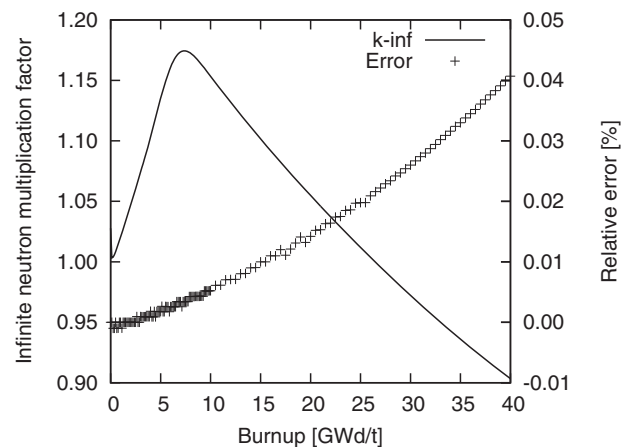


Figure 6. Infinite neutron multiplication factor and its reproduction errors in multi-cell problem including gadolinium-bearing fuel.

ditions, is prepared. Fuel compositions, geometric specifications and burnup conditions are taken from the Maeder BWR benchmark [10]. Maximum values and RMS of reproduction errors of the target NNDs at 40 GWd/t are 0.037% and 0.012%, respectively. These reproducibilities are consistent with those in the UO<sub>2</sub> cell calculations shown in the preceding calculations, so applicability of the 138-chain to NNDs prediction of the gadolinium-bearing fuel is confirmed. Reproduction errors of infinite neutron multiplication factor during burnup are also quantified as shown in Figure 6. Overestimation of reactivity is less than 0.05% till the 40 GWd/t burnup.

## 5. Conclusion

A method of identifying important FP nuclides which is included in a simplified burnup chain has been proposed. This method utilizes adjoint nuclide number densities and contribution functions which quantify the importance of nuclide number densities during burnup to the target nuclear characteristics. This method has been tested against LWR fuel pin-cell problems, and it has been shown that this method successfully identifies important FP nuclides to reproduce NNDs of the target nuclides with a simplified burnup chain. A



simplified burnup chain consisting of 138 FP nuclides is constructed using the proposed method, and its good performance for predictions of nuclide number densities of target nuclides and reactivity has been demonstrated against LWR pin-cell problems and multi-cell problem including gadolinium-bearing fuel rod.

Although each FP nuclide dropped from a simplified burnup chain has small contribution to reactivity, the sum of them cannot be neglected. Hence, a pseudo FP nuclide seems to be necessary to accurately calculate reactivity during burnup. A strategy to produce a pseudo FP nuclide should be considered in a future study.

### Acknowledgements

The authors wish to express their gratitude to Mr Y. Kawamoto of Hokkaido University for his support in the development of the CBZ burnup calculation capability.

### Disclosure statement

No potential conflict of interest was reported by the authors.

### References

- [1] Gandini A. Time-dependent generalized perturbation theory for burn-up analysis. Rome (Italy): *CNEN RT/FI(75)4*, Comitato Nazionale per l'Energia Nucleare; (1975).
- [2] Williams ML. Development of depletion perturbation theory for coupled neutron/nuclide fields. *Nucl Sci Eng.* 1979;70:20–36.
- [3] Takeda T, Umamo T. Burnup sensitivity analysis in a fast breeder reactor part I: sensitivity calculation method with generalized perturbation theory. *Nucl Sci Eng.* 1985;91:1–10.
- [4] Katakura J, Kataoka M, Suyama K, Jin T, Ohki S. A set of ORIGEN2 cross section libraries based on JENDL-3.3 library: ORLIBJ33 [in Japanese]. Ibaraki (Japan): Japan Atomic Energy Research Institute; 2004. (JAERI-Data/Code 2004-015).
- [5] Kawamoto Y, Chiba G, Tsuji M, Narabayashi Y. Validation of CBZ code system for post irradiation examination analysis and sensitivity analysis of (n, $\gamma$ ) branching ratio. In: Nakajima K, et al., editors. Proceedings of the 2012 Annual Symposium on Nuclear Data (NDS 2012) (JAEA-Conf 2013-002); 2012 Nov 15–16. Ibaraki (Japan): Japan Atomic Energy Agency; 2013; p. 113–118.
- [6] Katakura J. JENDL FP decay data file 2011 and fission yields data file 2011. Ibaraki (Japan): Japan Atomic Energy Agency; 2011. (JAEA-Data/Code 2011-025).
- [7] Shibata K, Iwamoto O, Nakagawa T, Iwamoto N, Ichihara A, Kunieda S, Chiba S, Furutaka K, Otuka N, Oh-sawa T, Murata T, Matsunobu H, Zukeran A, Kamada S, Katakura J. JENDL-4.0: a new library for nuclear science and engineering. *J Nucl Sci Technol.* 2011;48:1–30.
- [8] Chiba G, Okumura K, Oizumi A, Saito M. Sensitivity analysis of fission product concentrations for light water reactor burned fuel. *J Nucl Sci Technol.* 2010;47:652–660.
- [9] Okumura K, Kugo T, Kaneko K, Tsuchihashi K. SRAC2006: a comprehensive neutronics calculation code system. Ibaraki (Japan): Japan Atomic Energy Agency; 2007. (JAEA-Data/Code 2007-004).
- [10] Maeder C, Wydler P. International comparison calculations for a BWR lattice with adjacent gadolinium pins. Paris (France): Organization for Economic Co-operation and Development; 1984. (NEACRP-L-271).